

# Application of Continuous Wavelet Transform for Fault Location in Combined Overhead Line and Cable Distribution Networks

Behnam Feizifar<sup>1</sup>, Mahmoud Reza Haghifam<sup>2</sup>, *Senior Member, IEEE*, Soodabeh Soleymani<sup>1</sup>

<sup>1</sup>Department of Electrical Engineering, Islamic Azad University Tehran Science & Research Branch, Tehran, Iran  
zeroc\_cpp@yahoo.com, ssoleymani@srbiau.ac.ir

<sup>2</sup>Department of Electrical Engineering, Tarbiat Modares University, Tehran, Iran  
haghifam@modares.ac.ir

## Abstract

**This paper illustrates the application of continuous wavelet transform (CWT) for fault location in combined overhead line and cable distribution networks. The high frequency transient signals originated by faults are analyzed using CWT. The transient voltage waveform of faults is recorded at the certain measuring point. This method is based on the relationship between typical frequencies of the CWT signal energy and certain paths in the network passed by the travelling waves produced by faults. Due to this relationship, determination of the continuous frequency spectrum of fault transients in the form of signal energy is necessary and using characteristic frequencies directly related to the previously mentioned paths finally results in fault location. The IEEE 34-bus test distribution network is completely simulated in EMTP-RV and the CWT analysis of transient signals is implemented in MATLAB.**

## 1. Introduction

The reliability of distribution networks has been one of the most important issues of power industries in recent years. The amount and duration of short and long interruptions depend on the annual number of faults and on the relevant restoration times. In order to minimization of restoration times, the ability to calculate the accurate fault location is absolutely crucial [1]. The review of fault location approaches in distribution networks demonstrates the gravity of this subject in the literatures to maintain service continuity utmost. These techniques generally categorize into the following items:

- 1) Impedance measurement (e.g., [10]-[12]);
- 2) Analysis of fault transient signals.

Furthermore, the combination of neural networks and fault location methods has been also presented (e.g., [13]-[15]). Especially a methodology based on neural networks is proposed as a fault locator in power distribution lines. The main feature for training the artificial neural network is energy percentage in each level of the decomposed transient voltage signal obtained by a wavelet filter [9]. Impedance measurement-based methods rely essentially on the analysis at fundamental power frequency of voltage and current fault signals. These techniques are so functional in transmission lines due to their significant line length and simple network topology. Using these impedance measurement methods may decrease the location accuracy in a multi branched radial configuration. Recently, a novel fault location algorithm for overhead distribution networks giving an

integrated solution that omits or reduces iterative procedures, effective on all types of faults based on the bus impedance matrix has been presented [16]. On the other hand, travelling wave methods measure high frequency components of a signal by applying the complex signal analysis techniques. They analyze the high frequency components of fault transients, which are relatively independent of the fault type and impedance [7]. These methods considering the discrete wavelet transform as a signal analysis technique have been already proposed in distribution networks (e.g., [17], [8]). The integrated time-frequency wavelet decompositions of the voltage transients originated by the fault travelling waves have been also used in distribution systems. Moreover, the proposed analysis of time-frequency wavelet decompositions improves the identification accuracy of the frequencies associated to the characteristic patterns of a fault location in comparison to a sole frequency-domain wavelet analysis [6].

The method will be discussed later in this paper belongs to the second above mentioned category. Voltage waveform transients of the low voltage terminals of the transformer feeding the distribution network are recorded and analyzed using continuous wavelet transform (CWT). The continuous wavelet analysis is aimed at identifying characteristic frequencies associated to the faulted branch and to the fault location. In this paper, the Morlet-wavelet, one of the several traditional mother wavelets presented in the literature has been used (e.g., [18]-[19]). It is worth noting that, the mother wavelet of CWT can be chosen arbitrarily on condition that it satisfies the so-called "admissibility condition" [4].

## 2. Proposed combined theoretical approach

As known, the fault transient signals have time-variant characteristics with a continuous spectrum in the frequency domain. Consequently, using traditional transforms, such as fast Fourier transform (FFT) is absolutely inadequate for detecting the characteristic frequencies. Conversely, the wavelet transform allows the adjustment of the signal spectrum versus time. As a result, the continuous wavelet transform is an appropriate signal analysis tool for identification of the characteristic frequencies. Considering a radial distribution network topology, a definite number of paths can be seen from measurement point where the voltage waveform is recorded. Adding the number of network laterals and the number of feeder lateral junctions gives the number of above mentioned paths. As an example, figure 1 illustrates a portion of the IEEE 34-bus test distribution network which is completely simulated as a case study.

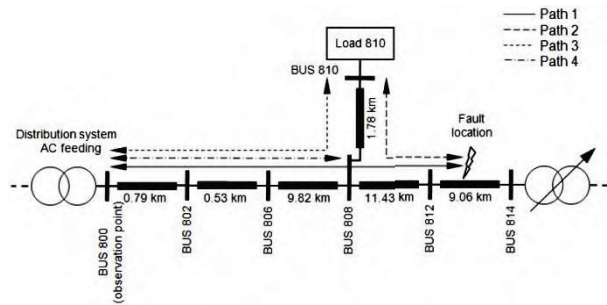


**Fig. 1.** Identified paths in a portion of the IEEE 34-bus test feeder caused by a fault between buses 812 and 814.

As it can be seen from fig. 1, there are four different paths covered by travelling waves but path number 2 is independent of observation point. Each path can be associated to a number of characteristic frequencies, one for each of the travelling wave propagation modes [20], [21]. Assume that the network configuration and the travelling wave of the various propagation modes are known, frequency  $f_{p,i}$  of mode  $i$  through path  $p$  can be calculated as

$$f_{p,i} = \frac{v_i}{n_p L_p} \quad (1)$$

where  $v_i$  is the travelling velocity of the  $i$ th propagation mode,  $L_p$  is the length of the  $p$ th path and  $n_p$  ( $\in \mathbb{N}$ ) is the number of times needed for a given travelling wave to move along path  $p$  before attain again the same polarity.  $p-1$  values are used to assess the faulted section and the last one to determine the fault distance between observation point and fault location. The reflection coefficient of the travelling waves in the network according to the extremities considered as follow:

- Extremities with a power transformer connection can be treated as open circuits, therefore, the relevant reflection coefficient is close to +1;
- Extremities associated to a junction between more than two lines have a negative reflection coefficient;
- The reflection coefficient of the extremity in the fault location is close to -1; because the fault impedance is lower than the line surge impedance.

The coefficient  $n_p$  depends on the sign of the reflection coefficients of the two path extremities; indeed  $n_p$  is equal to 2 or 4 if the reflection coefficients have the same or opposite sign, respectively.

Combined networks which comprise overhead lines and cables encounter different propagation velocities due to the different characteristics of two environments. The proposed idea is the calculation of an equivalent frequency associated to a certain path. As an instance, considering a path includes two sections (line and cable), the theoretical equivalent frequency according to equation 1 is as follow

$$\frac{1}{f_{eq,p,i}} = \frac{1}{f_{L,p,i}} + \frac{1}{f_{C,p,i}} = \frac{n_{p,L} L_{p,L}}{v_{i,L}} + \frac{n_{p,C} L_{p,C}}{v_{i,C}} \quad (2)$$

where

- $f_{eq,p,i}$  is the equivalent frequency of mode  $i$  through path  $p$ ;
- $f_{L,p,i}$  is the line frequency of mode  $i$  through path  $p$ ;
- $f_{C,p,i}$  is the cable frequency of mode  $i$  through path  $p$ ;
- $n_{p,L}$ ,  $L_{p,L}$ ,  $v_{i,L}$  and  $n_{p,C}$ ,  $L_{p,C}$ ,  $v_{i,C}$  are the same parameters as

equation 1 for the line and cable sections, respectively.

The equation 2 can be easily extended to a general formula which involves a path includes  $m$  line and  $n$  cable sections.

$$\frac{1}{f_{eq,p,i}} = \frac{1}{f_{L1,p,i}} + \frac{1}{f_{L2,p,i}} + \dots + \frac{1}{f_{Lm,p,i}} + \frac{1}{f_{C1,p,i}} + \frac{1}{f_{C2,p,i}} + \dots + \frac{1}{f_{Cn,p,i}} \quad (3)$$

### 3. Transient signals processing procedures

As previously mentioned, the identifying of characteristic frequencies must be performed by using appropriate signal analysis tools that allow the adjustment of the signal spectrum versus time. Generally, time frequency representations (TFRs) are the signal analysis techniques that link a one-dimensional time signal  $x(t)$  to a bi-dimensional function of time and frequency  $T_x(t,f)$ .

The numerical implementation of the CWT applied to the analyzed part  $s(t)$  of the recorded signal  $x(t)$ , which in our case associates to a first portion of the recorded voltage fault transient, gives a matrix  $C$  whose element are

$$C(a,b) = C(a, iT_s) = T_s \frac{1}{\sqrt{a}} \sum_{n=0}^{N-1} \left[ \varphi^* \left( \frac{nT_s - iT_s}{a} \right) s(nT_s) \right] \quad (4)$$

where:

- $T_s$  is the sampling time and  $N$  is the number of recorded samples of  $s(t)$ ;
- $a$  is the so-called scale factor;
- $b = iT_s$  is the so-called time shifting factor and  $i$  is an integer value.
- $\varphi(a,b)^*$  is the complex conjugate of the so-called daughter wavelet  $\varphi$ , which is a time translated and scale expanded or compressed version of a finite energy function  $\Phi(t)$ , called a mother wavelet.

Finally, coefficients  $C(a,b)$  represent a bi-dimensional function of time and frequency.

The sum of the squared values of all coefficients associated to the same scale, which are called CWT signal energy, illustrates a so-called "scalogram" which provides the weight of each frequency component [22].

$$E_{CWT}(a) = \sum_{n=0}^{N-1} (C(a, nT_s))^2 \quad (5)$$

Energy spectrum of the fault transient signal has high density around the path characteristic frequencies. Therefore, the detection of characteristic frequencies relevant to the fault location is performed by inspecting the relative maximum peaks of the obtained scalogram. For each fault location, some theoretical frequency values are calculated as a function of the length of the path passed by the travelling waves, of the propagation velocities along the overhead lines and cables and of the type of reflections. As known, the admissibility condition for choosing a mother wavelet is

$$C_h = \int_{-\infty}^{+\infty} \frac{|\varphi(\omega)|^2}{\omega} d\omega < \infty \quad (6)$$

which is satisfied by the two following conditions:

- Mean value of  $\varphi(t)$  equal to zero;
- Fast decrease to zero of  $\varphi(t)$  for  $t \rightarrow \pm\infty$ .

Comparing the theoretical characteristic frequency values and the CWT identified frequencies give us useful information about the fault location.

#### 4. Case study 1: Balanced solid faults

The proposed fault location approach is applied to the case of a three-phase balanced solid fault at bus 812 of the IEEE 34-bus distribution network simulated in the EMTP-RV environment. The simulation sampling period of the EMTP model is equal to 0.2  $\mu$ sec. Locating the observation point  $m$  at bus 800 (the medium voltage side of the feeding transformer) and the fault at bus 812, three travelling waves exist in the fault transient signal. They are characterized by a common path-terminal, bus 800, and other three path-terminals corresponding to buses 812 (path 1), 808 (path 2) and 810 (path 3). The first section of fig. 2 shows the fault voltage transient waveform of the propagation mode 1 observed at bus 800 of the IEEE 34-bus distribution system for a three-phase solid fault at bus 812, the second section illustrates the so-called Morlet-wavelet which has [-4 4] as effective support and the last section represents results of the CWT analysis of the mode 1 of the voltage transient signal. The values of the CWT signal energy are in per-unit with respect to the maximum. From fig. 2, the CWT is able to detect the frequencies associated to paths number 1 and 3. The frequency of path number 2 is hidden by the other frequency due to the large filter amplitude related to the adopted mother wavelet. The relevant results are shown in table 1.

Back to equation 5, the CWT signal energy is expressed as a function of scales. A probable question is that “How does one map a scale, for a given wavelet and a sampling period, to a kind of frequency?”

The answer can only be given in a broad sense and it is better to talk about the pseudo-frequency associating to a scale. A way to do it is to calculate the center frequency,  $F_c$ , of the wavelet and using the following relationship [25].

$$F_a = \frac{F_c}{a \cdot \Delta} \quad (7)$$

where

- $a$  is a scale;
- $\Delta$  is the sampling period;
- $F_c$  is the center frequency of a wavelet in Hz;
- $F_a$  is the pseudo-frequency corresponding to the scale  $a$ , in Hz.

The location error is defined as

$$e\% = \frac{100}{L_{p^*}} \left| L_{p^*} - \frac{v_i}{n_{p^*} \times f_{p^*,i}^{CWT}} \right| \quad (8)$$

where  $L_{p^*}$  is the length of path  $p^*$  between the observation point and fault location,  $v_i$  is the propagation velocity of mode  $i$ ,  $n_{p^*}$  is equal to 4 and  $f_{p^*,i}^{CWT}$  is the CWT identified frequency corresponded to path  $p^*$  [3].

To be guaranteed the CWT backward transformation (equation 9), i.e., the signal reconstruction, choosing the number and

spacing of scale  $a$  along with the choice of the mother wavelet, should satisfy the so-called orthogonality condition (e.g., [24]), which is

$$f(t) = \frac{1}{C_\varphi} \int_{-\infty}^{+\infty} \int_{-\infty}^{+\infty} C(a, b) \varphi_{a,b}(t) \frac{da db}{a^2} \quad (9)$$

**Table 1.** Theoretical and CWT-identified characteristic frequencies relevant to the propagation mode 1 for a three-phase solid fault located at bus 812 of fig. 1.

Path	Path length $n_p \cdot L_p$ (km)	Theoretical frequencies $f_{p,i}$ (propagation of mode1) (kHz)	CWT identified frequency (kHz)
800-812	4x22.57	3.29	3.98
800-808	4x11.14	6.68	-
800-810	2x12.92	11.52	10.13

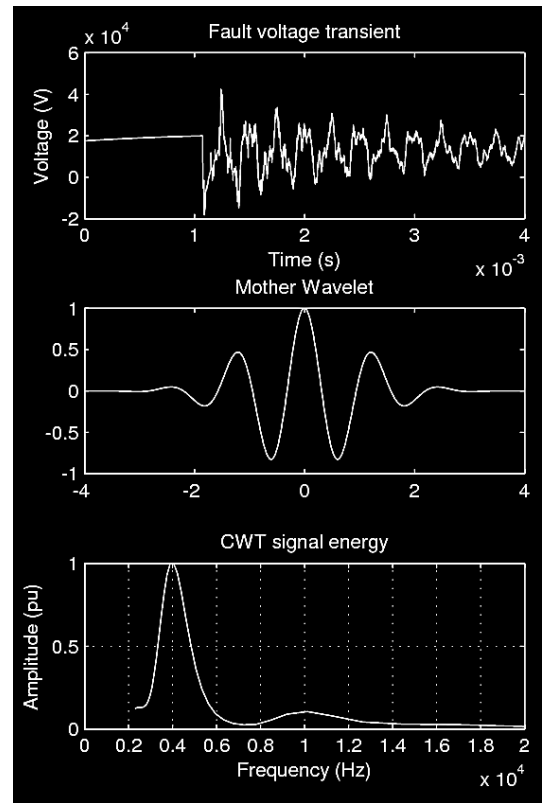


**Fig. 2.** Fault voltage transient, Morlet-wavelet and relevant CWT signal energy of the IEEE 34-bus test distribution network with a fault located at bus 812.

The CWT used in the proposed fault location method does not need to satisfy the orthogonality condition which is essential if time-domain fault location approaches (e.g., [7], [8]), based on reconstruction of the fault transient signal related to each characteristic frequency, were adopted. As another example, for a three-phase solid fault located at bus 814 of the IEEE 34-bus test distribution system, the relevant CWT signal energy is shown in fig. 3 and the characteristic frequencies are reported in table 2. In order to simplicity: 1) all the branches of the network are modeled by overhead lines. The conductor configuration is the “ID #500” according to [23, Fig. 1]; 2) the network loads are

assumed located in the line terminations. The power distribution transformers are modeled by means of the 50 Hz parallel standard model and a  $\Pi$  of capacitances aimed at representing, in a first approximation, its response to the transients at the frequency range around 100 kHz, as shown in fig 4.

**Table 2.** Theoretical and CWT-identified characteristic frequencies relevant to the propagation mode 1 for a three-phase solid fault located at bus 814 of fig. 1.

Path	Path length $n_p \cdot L_p$ (km)	Theoretical frequencies $f_{p,i}$ (propagation of mode1) (kHz)	CWT identified frequency (kHz)
800-814	4x31.63	2.35	3.02
800-808	4x11.14	6.68	7.24
800-810	2x12.92	11.52	-

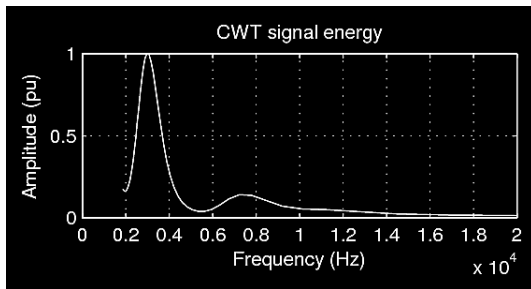


**Fig. 3.** CWT signal energy of the IEEE 34-bus test distribution network with a fault located at bus 814.

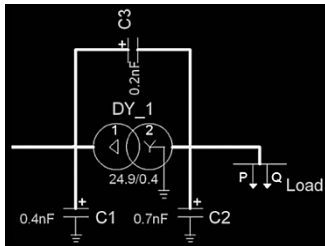


**Fig. 4.** Transformer model implemented in EMTP

The parameters of the 50 Hz parallel standard transformer models are as follow:

- 5 MVA      150/24.9 kV  $V_{sc}=9\%$  for the substation;
- 1 MVA      24.9/0.4 kV  $V_{sc}=4\%$  for the loads and,
- 2.5 MVA    24.9/24.9 kV  $V_{sc}=8\%$  for the regulators.

A constant parameter line model (CP-line model) has been used for the overhead lines. Table 4 shows the modal parameters of the CP-line model referring to the considered overhead line configuration. The modal parameters are calculated for the frequency of 1 kHz and ground resistivity equal to 100  $\Omega m$ .

### 5. Case study 2: Combined distribution networks

To verifying the application of the proposed algorithm for fault location in combined overhead line and cable distribution networks, the line between buses 808 and 810 is replaced by a typical distribution cable (with the same size and length) in the relevant EMTP-RV model. In this case the three-phase solid fault is located at bus 810. The CWT and theoretical characteristic frequencies for both case studies are shown in

table 3. The CWT signal energy of the IEEE 34-bus test distribution system for the fault located at bus 810 in cases number 1 and 2 are shown in fig. 5 and 6, respectively.

**Table 3.** Theoretical and CWT-identified characteristic frequencies relevant to the propagation mode 1 for a three-phase solid fault located at bus 810 of fig. 1.

Case No.	Path	Path length $n_p \cdot L_p$ (km)	Theoretical frequencies $f_{p,i}$ (propagation of mode1) (kHz)	CWT identified frequency (kHz)
1	800-810	4x12.91	5.76	6.99
2	800-810	4x11.14 4x1.77	5.45	6.76

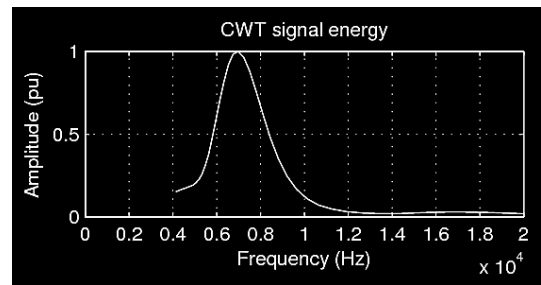


**Fig. 5.** CWT signal energy of the IEEE 34-bus test distribution network with a fault located at bus 810 applied in case study number 1.

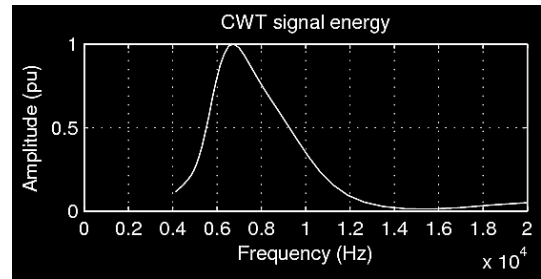


**Fig. 6.** CWT signal energy of the IEEE 34-bus test distribution network with a fault located at bus 810 applied in case study number 2.

It can be observed that the characteristic frequency obtained by the case study number 1 is higher than case study number 2, due to different velocities between two environments (overhead lines and cables) as described in section 2.

**Table 4.** Modal parameters calculated at 1 kHz and ground resistivity equal to 100  $\Omega m$  for propagation mode 1.

R ( $\Omega/km$ )	L (mH/km)	C ( $\mu F/km$ )	$Z_c$ ( $\Omega$ )	Propagation Speed (km/s)
0.136	0.908	$1.243 \times 10^{-2}$	270.27	$2.976 \times 10^5$

### 6. Conclusion

An effective fault location algorithm for combined overhead line and cable distribution networks has been presented which is based on the CWT analysis of high frequency components of

transient signals associated to the travelling wave phenomena occurring after a fault event. Principally, due to the fact that traditional mother wavelets do not have ability to identify all the characteristic frequencies of the travelling waves originated by faults, coupled with the relevant path, associated to a specific fault location, finding an appropriate mother wavelet would be crucial. Additional research activities will be devoted to improve the accuracy of the proposed algorithm by definition of a transient inferred mother wavelet with maximum similarity to the fault transients. Further studies involve some external factors, type of faults, their impedance and position, type of lines and cables, junctions, jumpers and many other accessories in distribution networks.

## 7. Appendix

The configuration of overhead line and cable simulated in EMTP-RV are shown in fig. 7.

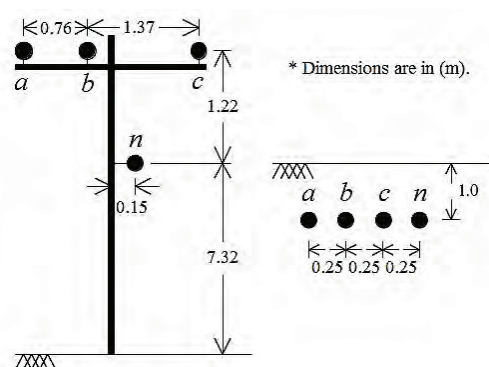


Fig. 7. Configuration of the a) overhead line and b) cable.

## 8. References

- [1] *Fault Management in Electrical Distribution Systems*, CIRED WG03 Fault Management, 1998.
- [2] *IEEE Std C37.114, IEEE Guide for Determining Fault Location on AC Transmission and Distribution Lines*, 2004.
- [3] A. Borghetti, M. Bosetti, M. Di Silvestro, C. A. Nucci, and M. Paolone, "Continuous-wavelet transform for fault location in distribution power networks: Definition of mother wavelets inferred from fault originated transients," *IEEE Trans. Power Syst.*, vol. 23, no. 2, pp. 380–388, May 2008.
- [4] A. Borghetti, S. Corsi, C. A. Nucci, M. Paolone, L. Peretto, and R. Tinarelli, "On the use of continuous-wavelet transform for fault location in distribution power networks," *Elect. Power Energy Syst.*, vol.28, pp. 608–617, 2006.
- [5] A. Borghetti, M. Bosetti, C. A. Nucci, M. Paolone, "Fault location in active distribution networks by means of the continuous-wavelet analysis of fault originated high frequency transients" *CIGRE*, 21, rue d'Artois, F-75008 PARIS, 2010.
- [6] A. Borghetti, M. Bosetti, C. A. Nucci, M. Paolone, A. Abur, "Integrated use of time-frequency wavelet decompositions for fault location in distribution networks: Theory and experimental validation," *IEEE Trans. Power Del.*, vol. 25, no. 4, pp. 3139–3146, Oct. 2010.
- [7] F. H. Magnago and A. Abur, "Fault location using wavelets," *IEEE Trans. Power Del.*, vol. 13, no. 4, pp. 1475–1480, Oct. 1998.
- [8] F. H. Magnago and A. Abur, "A new fault location technique for radial distribution systems based on high frequency signals," in *Proc. IEEE-Power Eng. Soc. Summer Meeting*, Jul. 18–22, 1999, vol. 1, pp. 426–431.
- [9] M. P. Nakhli, A. A. Safavi, "Path characteristic frequency-based fault locating in radial distribution systems using wavelets and neural networks," *IEEE Trans. Power Del.*, vol. pp, no. 99, pp. 1–10, Jun. 2010.
- [10] M. S. Sachdev and R. Agarwal, "A technique for estimating transmission line fault locations from digital impedance relay measurements," *IEEE Trans. Power Del.*, vol. 3, no. 1, pp. 121–129, Jan. 1988.
- [11] K. Srinivasan and A. St-Jacques, "A new fault location algorithm for radial transmission lines with loads," *IEEE Trans. Power Del.*, vol. 4, no. 3, pp. 1676–1682, Jul. 1989.
- [12] A. A. Girgis, D. G. Hart, and W. L. Peterson, "A new fault location technique for two- and three-terminal lines," *IEEE Trans. Power Del.*, vol. 7, no. 1, pp. 98–107, Jan. 1992.
- [13] S. Ebron, D. L. Lubkeman, and M. White, "A neural network approach to the detection of incipient faults on power distribution feeders," *IEEE Trans. Power Del.*, vol. 5, no. 2, pp. 905–914, Apr. 1990.
- [14] Z. Chen and J. C. Maun, "Artificial neural network approach to single ended fault locator for transmission lines," *IEEE Trans. Power Syst.*, vol. 15, no. 1, pp. 370–375, Feb. 2000.
- [15] N. Kandil, V. K. Sood, K. Khorasani, and R. V. Patel, "Fault identification in an AC-DC transmission system using neural networks," *IEEE Trans. Power Syst.*, vol. 7, no. 2, pp. 812–819, May 2002.
- [16] Y. Liao, "Generalized fault-location methods for overhead electric distribution systems," *IEEE Trans. Power Del.*, vol. 26, no. 1, pp. 53–64, Jan. 2011.
- [17] O. Chaari, M. Meunier, and F. Brouaye, "Wavelets: A new tool for the resonant grounded power distribution systems relaying," *IEEE Trans. Power Del.*, vol. 11, no. 3, pp. 1301–1308, Jul. 1996.
- [18] P. Goupillaud, A. Grossmann, and J. Morlet, "Cycle-octave and related transforms in seismic signal analysis," *Geoexploration*, vol. 23, pp. 85–102, 1984–1985.
- [19] O. Rioul and M. Vetterli, "Wavelets and signal processing," *IEEE Signal Process. Mag.*, vol. 8, no. 4, pp. 14–38, Oct. 1991.
- [20] E. Clarke, *Circuit Analysis of AC Power Systems*, 1. New York: Wiley, 1943.
- [21] H. W. Dommel, "Digital computer solution of electromagnetic transients in single and multi-phase networks," *IEEE Trans. Power App. Syst.*, vol. PAS-88, pp. 388–399, Apr. 1969.
- [22] T. Lobos, T. Sikorski, and P. Schegner, "Joint time-frequency representation of non-stationary signals in electrical power engineering," in *Proc. 15th Power Systems Computation Conf. (PSCC'05)*, Liege, Belgium, Aug. 22–26, 2005, paper fp 97.
- [23] IEEE Distribution Planning Working Group, "Radial distribution test feeders," *IEEE Trans. Power Syst.*, vol. 6, no. 3, pp. 975–985, Aug. 1991.
- [24] G. Strang and T. Nguyen, *Wavelets and Filter Banks*. Wellesley, MA: Wellesley Cambridge Press, 1996.
- [25] *Matlab Wavelet Toolbox, User's Guide*, MathWorks, 1997.